Experimental Study on Flexural Strengthening of RC Columns with Near Surface Mounted FRP Bars

M. Sarafraz [1*] and F. Danesh [2]

1. PhD in Structural Engineering, Civil Engineering Dept., K.N. Toosi University of Technology, Tehran, I.R. Iran,
* Corresponding Author; email: sarafraz@dena.kntu.ac.ir
2. Associate Professor, Civil Engineering Dept., K.N. Toosi University of Technology, Tehran, I.R. Iran

ABSTRACT

The effectiveness of FRP jackets for increasing the compression strength, shear strength and ductility of reinforced concrete (RC) columns was demonstrated in many studies, but the influence of FRP jacketing on the flexural capacity of columns is minimal. In this paper, a new retrofit method, which utilized near surface mounted (NSM) fiber reinforced polymer (FRP), was studied aiming to improve the flexural capacity of RC columns subjected to bending and compression. This technique is based on bonding fiber reinforced polymer (FRP) bars into grooves cut in the cover of RC columns. For this purpose, five reinforced concrete column specimens were designed, constructed and subjected to constant axial compression and lateral cyclic loading. In addition, the strengthened columns were wrapped with carbon composites to satisfy seismic detailing requirements. The test results show that by using the NSM technique, the flexural strength and lateral load capacity of the columns increase significantly. The test results were also compared with the results obtained from the analytical study that was conducted based on strain compatibility. A good agreement between analytical and experimental results was observed.

Keywords:
Flexural strengthening; Reinforced concrete column; NSM rod; FRP; Composite

1. Introduction

Many concrete structures are in need of strengthening due to new seismic codes requirements, structural deficiencies due to errors in calculation or plan execution, adaptation of a structure for a different function, and poor construction practices.

Retrofitting of reinforced concrete columns is of great importance in the rehabilitation of existing structures [1]. Flexural strength deficiency in *RC* columns may arise from the loss of reinforcement due to corrosion, premature termination of the main reinforcement, or inadequate splicing. The most common traditional methods for flexural strengthening of *RC* columns are concrete and steel jacketing. However, these systems may not be very practical due to undesirable section enlargement or construction constraints.

In recent years, Fiber-reinforced polymer (*FRP*) materials are increasingly used for strengthening and retrofitting of reinforced concrete structures. The main advantages of the *FRP* system for strengthening of *RC* structures include lightweight, noncorrosive and high-tensile strength of the *FRP* and these in turn provide a more flexible and economical technique than traditional techniques. Column jacketing with *FRP* composite materials has been extensively studied in the last few years to address the issue of seismic upgrade and retrofit of existing *RC* columns [2-7]. The *FRP* jackets however provide lateral confinement to concrete columns that can improve compression strength, shear strength, and ductility of the member, but it may not improve the flexural capacity of *RC* columns sufficiently.

Near surface mounted (*NSM*) *FRP* bars are another technique that could be used to improve the flexural capacity of *RC* columns. This strengthening technique consists of *FRP* rods embedded in grooves

made on the surface of the concrete and bonded in place with epoxy. *NSM* requires no surface preparation work and after cutting the slit, requires minimal installation time compared to the externally bonded reinforcing (*EBR*) technique [8-12].

Only a few research investigations are available that deal with *RC* columns strengthened in bending with *NSM FRP* bars. Barros et al [13] tested eight *RC* columns strengthened with *NSM* bars under cyclic flexure combined with axial load. The tests showed a good improvement of flexural strength of columns. Bournas and Triantafillou [14] investigated the behavior of eleven rectangular columns retrofitted by *NSM FRP* and steel bars under simulated seismic loading. Another innovative aspect in this study is the combination of *NSM* reinforcement with local jacketing, which comprised the textile-reinforce mortar (*TRM*) confining system. Test results showed that *NSM FRP* or steel reinforcement is a viable solution toward enhancing the flexural resistance of *RC* columns subjected to seismic loads.

In this work a strengthening technique, based on the installation of *NSM* bars was used to increase the flexural resistance of *RC* columns. To investigate the applicability and effectiveness of this technique, a test program was carried out. Flexural strengthening was achieved by inserting *NSM* rods on two opposite sides of the columns. In addition, the strengthened columns were wrapped with carbon composites to satisfy seismic detailing requirements. The columns were tested to failure by applying constant axial compressive and cyclic lateral loading. Also, an analytical model based on strain compatibility and internal force equilibrium was proposed to verify test results and to predict the columns' flexural strength. The accuracy of the proposed analysis was examined by comparing the analytical predictions with the experimental results of the present study. Good agreement between analytical and experimental results was observed.

2. Experimental Program

2.1. Specimens

Five column specimens of an approximately 1/3 scale were tested. Figure (1) shows the cross-sections of specimens. The columns with bottom and top reinforced concrete blocks were used to anchor the specimens to the reaction frame and applied the lateral and axial loads at the top of the columns, respectively. The column height of all specimens was 1000*mm* and the original cross-section was 200*mm* in width and depth. The volumetric ratio of the longitudinal steel reinforcement for the reinforced columns was 1.53%, consisting of four bars of 14*mm* diameter each. Steel stirrups were used as transverse reinforcement, having a diameter of 10*mm* and spaced at 100*mm* centers.

The following denominations are adopted: *C*1 for non-strengthened column; *C*2 for column strengthened with 2 *NSM* rods (one rod on two opposite sides

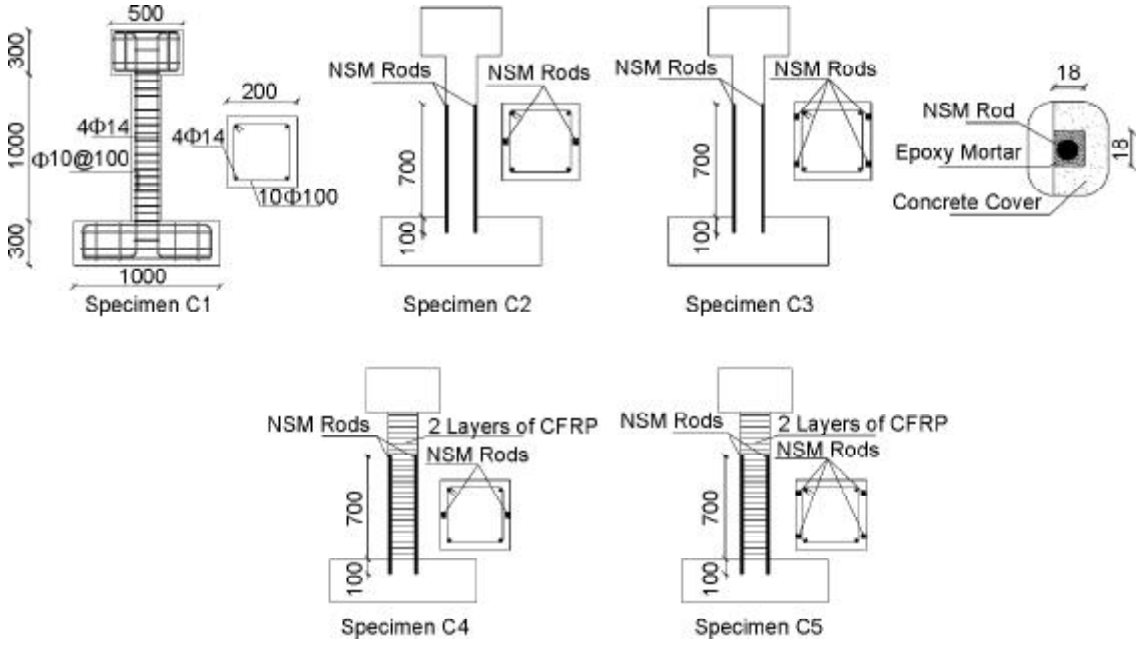

Figure 1. Dimensions, details of reinforcement, and strengthening for the specimens (Unit; mm).

of the column); *C*3 for column strengthened with 4 *NSM* rods (two rods on two opposite sides of the column). Columns *C*4 and *C*5 were retrofitted with two layers carbon *CFRP* jacketing plus the *NSM* embedment as that for columns *C*2 and *C*3.

In this study, the anchorage length of the *NSM* reinforcement was not an experimental parameter and a constant value of 100*mm* was initially selected. For anchoring the *NSM* bars, a hole with 100*mm* length and 18*mm* diameter in bottom block was created and the *NSM* rods were placed in the hole. Properties of the specimens are shown in Table (1).

2.2. Material Properties

Table (1) shows the main properties of the concrete used in the experimental program. The concrete compression strength was obtained from uniaxial compression tests with cylinder specimens of 150*mm* diameter and 300*mm* height at the time of testing. The nominal concrete strength at 28 days was 21*MPa*.

Columns were fabricated using steel with nominal yield stress of 400*MPa*. The average measured yield stress of the 14*mm* diameter longitudinal reinforcing bars was 410*MPa* and the average measured yield stress of the 10*mm* diameter transverse reinforcing bars was 380*MPa*. The mechanical properties of the *NSM* rods, *CFRP* jacketing and are epoxy pastes were provided by the manufacturer and presented in Table (2). The maximum bond strength of *NSM* rods based on pull out test performed using penn state method is 11.6*MPa*.

Table 1. Properties of specimens.

Specimen	Concrete Strength (MPa)	Retrofit Detail	ρ_{NSM}
C1	23.3	Unretrofitted	-
C2	22.7	NSM only	0.0039
C3	21.6	NSM only	0.0078
C4	20.3	NSM + Jacketing	0.0039
C5	23.1	NSM + Jacketing	0.0078

2.3. Test Setup and Loading Protocol

The test setup consisted of a reaction frame supporting the lateral and vertical hydraulic actuator. Figure (2) shows the test setup and details of the loading system. Specimens were constructed on a stiff base block to simulate rotational fixity of the columns. A pantograph system was installed to restrain the fixed end of the test column against rotation. A top block was provided to transfer the axial and lateral loads to the specimens. To prevent side-sway that might occur under large displacement, side-sway restraint was provided to ensure in-plane movement of the test columns.

Prior to the application of lateral load, the column was first loaded with a constant axial load of 200*kN* using a 500*kN* actuator centered on the top block of the specimens. This axial load corresponded approximately to 25% of the ultimate axial load carrying capacity. Under a sustained constant axial force, the 250*kN* servo controlled actuator applied the horizontal load to the test specimen in a displacement control mode in accordance with the predetermined loading history of Figure (3).

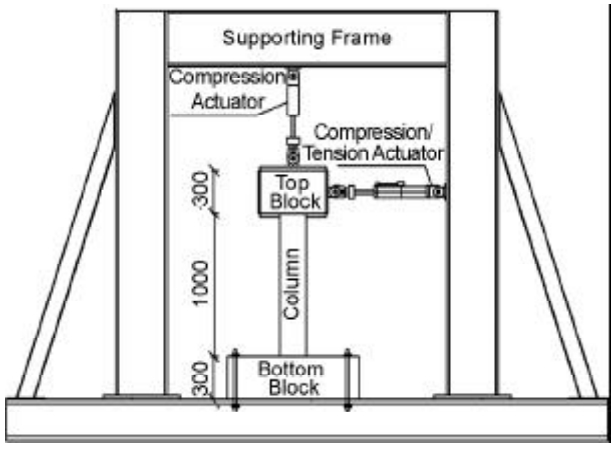

Figure 2. Test setup (Unit; mm).

Table 2. Properties of the NSM and CFRP composite materials.

Composite Type	Design Thickness (mm)	Design Diameter (mm)	Tensile Strength (MPa)	Tensile Modulus (GPa)	Ultimate Strain (%)
CFRP Sheet	0.176	-	3800	240	1.55
NSM Rod	-	10	760	40.8	1.6
Epoxy Mortar	-	-	27.6	3	1
Epoxy Resin	-	-	54	3	2.5

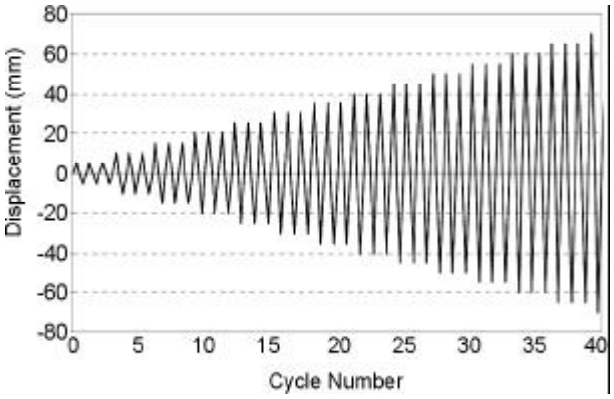

Figure 3. Loading history for the cyclic tests.

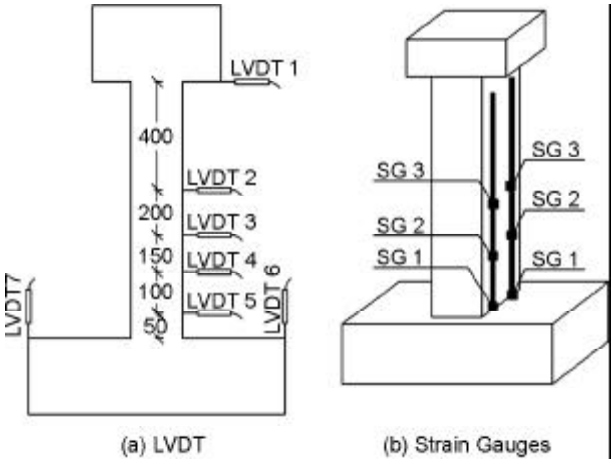

Figure 4. Details of instrumentation (Unit; mm).

For all specimens, the lateral cyclic displacement level was selected as multiples of $0.5\Delta y$. Three full cycles were applied at each load or displacement level before proceeding to the next predetermined level. The yield deflection Δy for control specimen was defined as the displacement at the top of the column when first yielding of the longitudinal bars occurs. From the analytical and numerical simulations for control specimen, it was verified that the steel yield initiation occurred for a lateral deflection of about 10*mm* at the level of the horizontal actuator. For comparison between specimens, the yield displacement was assumed equal to the measured displacement of the control specimen at the calculated yield load.

2.4. Instrumentation

Linear variable displacement transducers (*LVDTs*) were used to record the horizontal displacements of the column as well as any vertical movement of the footing, as shown in Figure (4a). Strains in the longitudinal reinforcement and *NSM* rods were measured using strain gauges. For each *NSM* rod, three strain gauges were placed at the bottom, 1/4 height and 1/2 height of each rod. The position of the strain-gauges (*SG*) glued on the *NSM* rod is indicated in Figure (4b). For each specimen, two strain gauges were placed on each of the four corner longitudinal bars and were located at the bottom and 1/3 height of each bar. Six strain gauges were placed on the outer surface of the *FRP* sheets; three gauges were at the centerline axis of the column while the other three were near the edge of the column and were located at the bottom, mid height and top end of the column.

2.5. NSM and CFRP Jacketing Application Procedures

The strengthening technique steps were as following:

Embedment of the rods was achieved by grooving the surface of the member to be strengthened along the desired direction. Continuity with foundation was obtained by drilling a hole into such member. The dust inside the holes was then removed with a vacuum cleaner. To bond the *NSM* rods to the column test series, an epoxy mortar was used. This epoxy mortar was composed of three parts of epoxy and one part of a hardening component (parts measured in weight). The groove was filled half way with epoxy mortar. The *NSM* rod was then placed in the groove and lightly pressed, forcing the paste to flow around the bar and fill completely between the bar and the sides of the groove. The groove was then filled with more mortar and the surface was leveled. The *NSM* strengthening techniques are represented in Figure (5). *NSM* installing was done before axial loading.

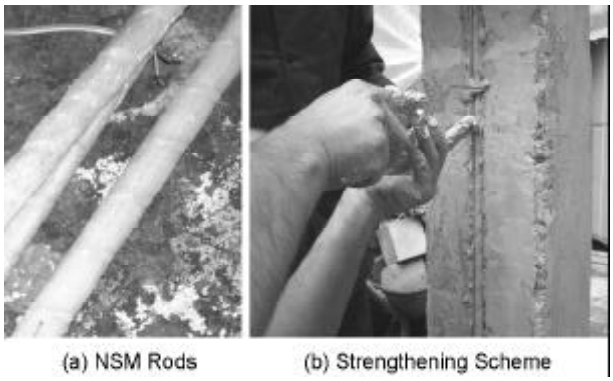

Figure 5. Strengthening techniques.

After completing the installation of *NSM* reinforcement, the *FRP* jacket was provided with the purpose of confining both concrete and rods in columns *C*4 and *C*5. Two layers of *CFRP* sheet were applied to these columns. Before jacketing, the sharp corners of columns were grinded to provide a corner radius of about 20*mm*. To guarantee the performance of *FRP* sheets, all four surfaces of these columns were cleaned to make the surfaces become smooth. In the construction of the jacket, the carbon sheets were saturated with the mixed epoxy resin; and a coat of epoxy resin was applied onto the prepared surfaces of the columns. The saturated fabrics were then wrapped around the column with fiber orientation in the circumferential direction. The jacket edge was located 5*mm* above the foundation block. The overlap length was 100 *mm*.

3. Experimental Results

3.1. Failure Modes and Crack Patterns

The tests were done according to the procedures described in Section 2.3. The failure mode of all tested specimens was controlled by flexure, due to their high ratio of transverse reinforcement and low ratio of longitudinal reinforcement. This was an important requirement to evaluate the effectiveness of *NSM* rod to flexural strengthening of *RC* columns. Observations during the first test in column *C*1 indicated that the first crack was formed at the tension side at 0.65% drift ratio. Drift ratio was calculated dividing the measured displacement at the center of the top block by the distance to the top face of the base block. The position of the first crack was about 100*mm* distance from the base of column. The cracks were widened during the subsequent cycles at the same displacement. At the 1.0% and 1.5% drift levels, new cracks appeared and continued to widen. As the lateral displacement reached a value of 1.8% of drift, the specimen reached the maximum capacity of lateral resistance strength. At 2.3% drift level, the cover concrete experienced extensive spalling. At this stage, the buckling of longitudinal bars was accomplished with the crushing of the concrete. The column lost its stability and severely damaged when the lateral displacement reached 5.4% drift. The test was ended with crushing of the concrete and buckling of longitudinal reinforcements, as shown in Figure (6a).

Specimens *C*2 and *C*3 showed a similar evolution of the cracking pattern and the same failure mechanism. These columns were tested to investigate the effect of *NSM* rod for flexural strengthening of column. The first flexural cracking occurred when the specimen was subjected to a drift level of 1% in specimen *C*1 and 1.1% in specimen *C*2. The lateral resistance reached the maximum value at the displacement of about 2.1% and 2.2% of drift, respectively. These specimens failed in bending with failure occurred by the splitting of epoxy paste simultaneously with the debonding of the *NSM* rods and separation of the *NSM* rods covers, see Figures (6b) and (6c). In all strengthened specimens, the buckling of the longitudinal bars occurred after debonding of the *NSM* rods. During testing, a crackling noise revealed the progressive cracking of the epoxy paste, until the epoxy cover was split and intersected by the major concrete crack, and the load decreased. The tests were halted when the specimens lost 50% of their ultimate capacity. Visual inspection after failure revealed that the splitting of epoxy paste was observed extensively near the crack to the column base, however, the other part of the epoxy paste remained intact.

Specimens *C*4 and *C*5 which were strengthened with *NSM* rod and *CFRP* jacket to investigate the combined effect of *NSM* bars and *CFRP* sheets jacketing, showed a similar evolution of the cracking pattern and the same failure mechanism. No apparent distress was shown except some very weak sound of epoxy cracking on the surface of the *CFRP* sheets. The lateral resistance reached the maximum value when the drift reached 2.2% in specimen *C*4 and 2.3% in specimen *C*5. The tests were halted when the specimens had lost more than 50% of their maximum lateral load carrying capacity. After the test, the *CFRP* wrapping was removed from the bottom parts of the columns. The concrete at the plastic hinge location was severely crushed and had several cracks. Also, the end region of *NSM* bars at the plastic hinge location was crushed in compression load, see Figure (6d). Compared with the specimens without *CFRP* jacketing, the peak force increased up to approximately 14% in specimen *C*4 and 10% in specimen *C*5. Therefore, jacketing with *CFRP* improved the bond conditions and restrained debonding of the *NSM* reinforcement and increased the strength capacity as well.

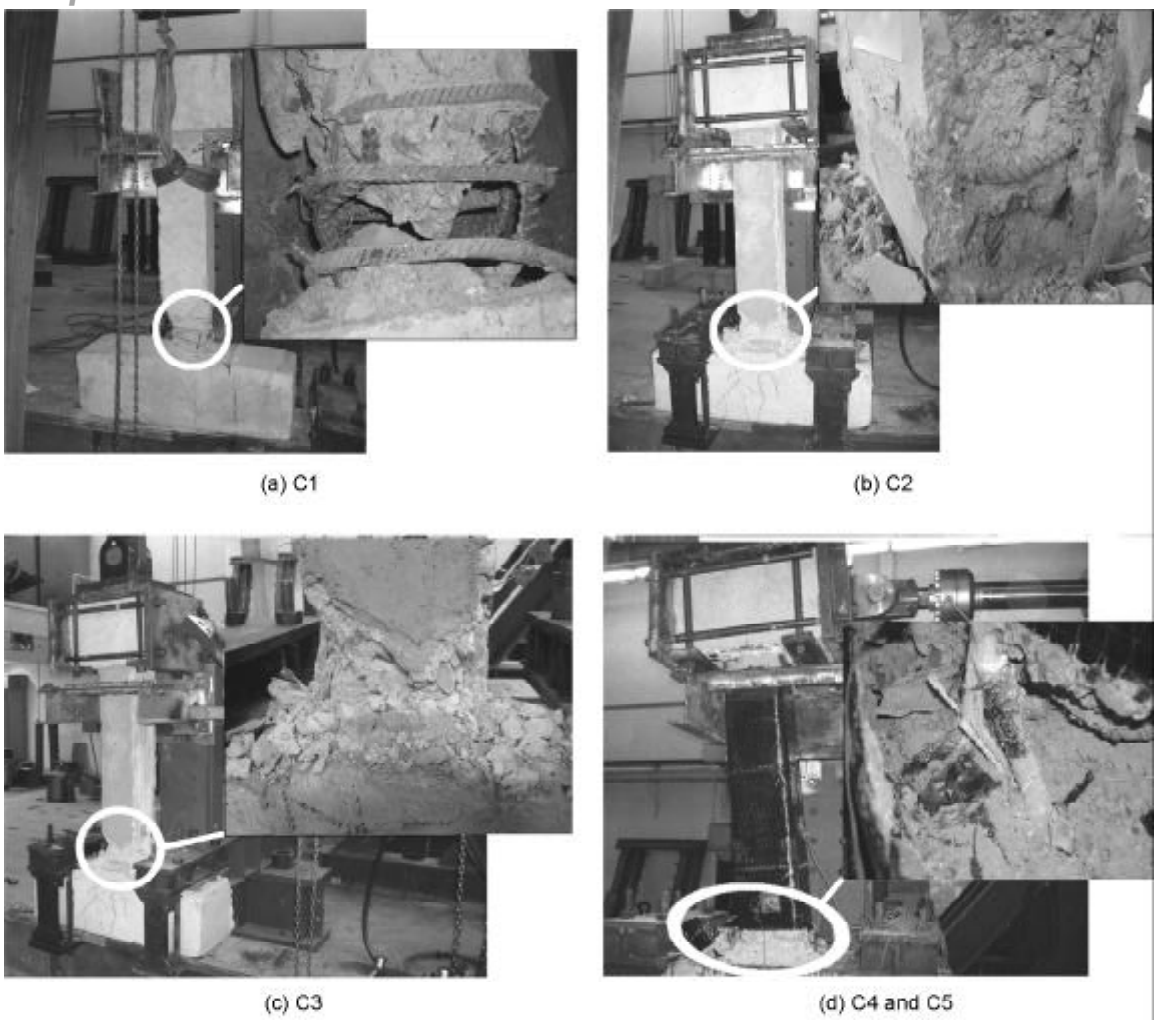

Figure 6. Test specimens at maximum lateral displacement.

3.2. Force-Displacement Relationship

Both the positive and negative peak points are given in Table (3). The response of specimens was not in all cases completely symmetrical in the two directions of loading. This is because the longitudinal reinforcement in the specimens was not ideally symmetrical regarding the cross section and also the differences may be due to the testing setup.

The lateral load-displacement relationships for specimens are plotted in Figure (7a) to (7e). The displacement is related to the top of the column. The lateral load is adjusted to include the contribution of the horizontal component of inclined axial load. In unstrengthened column (specimen *C*1), a pronounced pinching effect occurred (narrowing of the hysteretic diagrams) and indicated that this column had no capacity to dissipate energy.

Figure (8) compares the envelopes of load-displacement behavior of specimens. In general, columns with *NSM* rods showed an improvement in

Table 3. Summary of test results.

Specimen	Positive Peak Point		Negative Peak Point		Increase in Peak Force (%)	Ductility	Initial Stiffness (kN/mm)	Energy Dissipation (kN/m)
	F^{+}_{peak} (kN)	Δ^{+}_{peak} (mm)	F^{-}_{peak} (kN)	Δ^{-}_{peak} (mm)				
C1	18.8	19	19.2	19.6	-	2.4	4.82	14.93
C2	26.4	23	26.1	22.8	37	3.2	5.13	16.32
C3	34.6	23.5	34.2	23.1	80	2.8	5.21	18.79
C4	30.2	23.5	29.8	23.2	57	4.3	5.26	17.04
C5	37.8	24	38.9	23.6	102	4.2	5.31	22.1

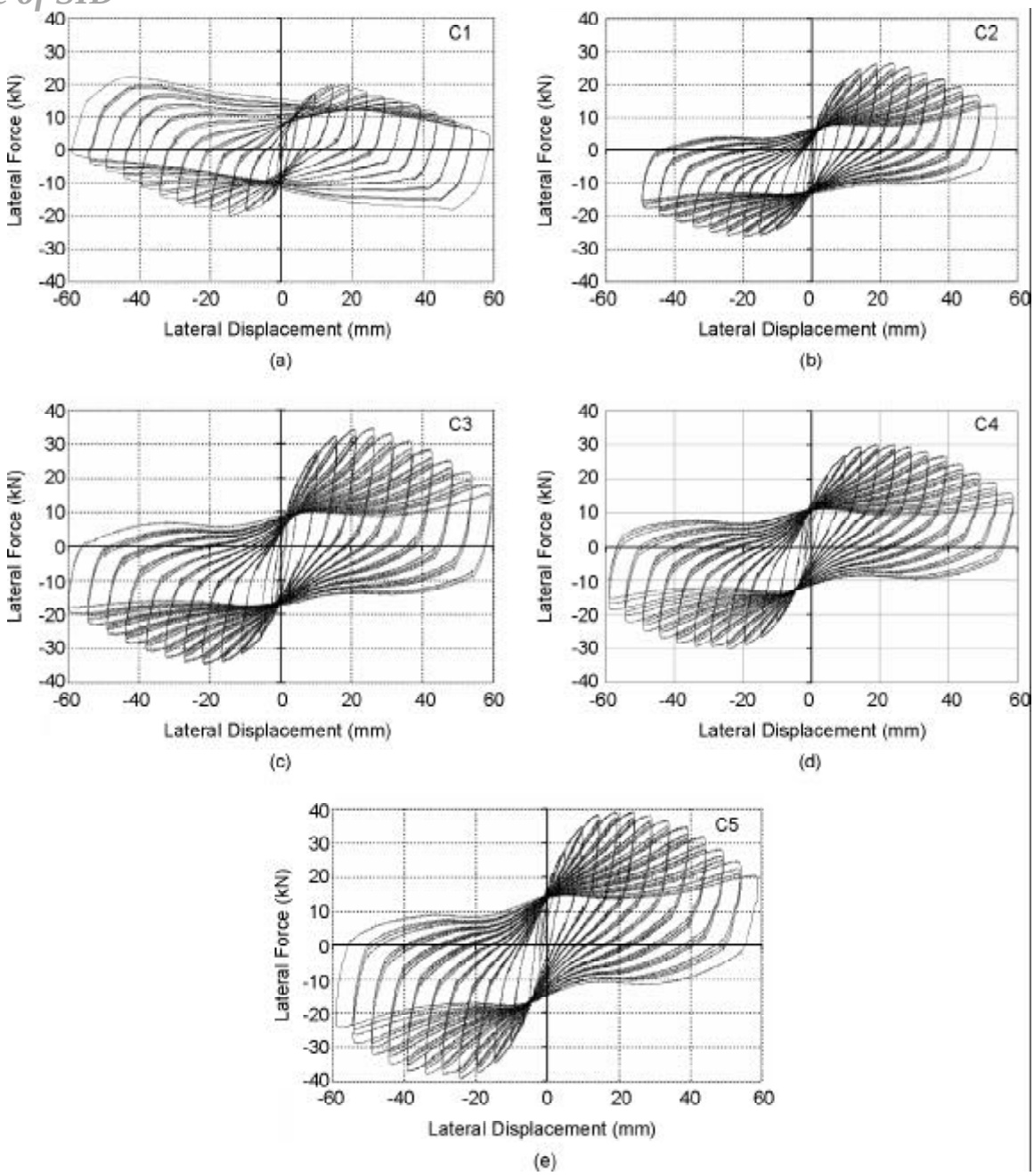

Figure 7. Comparison between the lateral force-displacement relationships for the specimens.

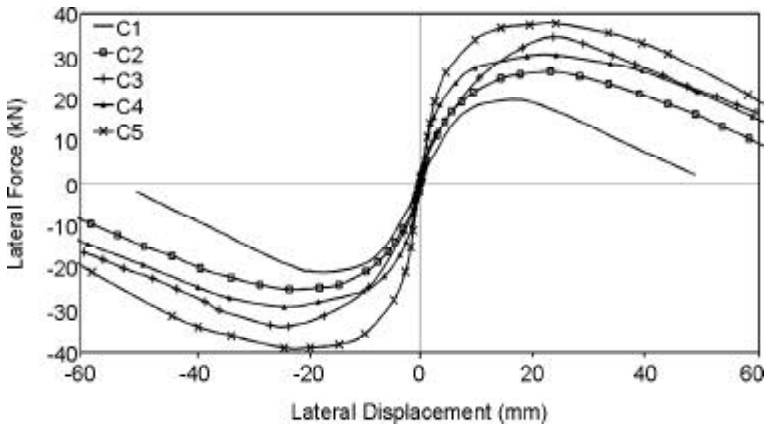

Figure 8. Envelope curves.

lateral strength capacity. From Table (3), specimen strengthened with more *NSM* rods, improved the overall lateral strength when compared to the similar specimen strengthened with less *NSM* rods. Increasing the *NSM* reinforcing ratio by 100% (two versus one bars in each side) increased the strength capacity that is from 37% in specimen *C*2 to 80% in specimen *C*3. Therefore, increasing the ratio of *NSM* rods, increased the column's lateral strength.

According to Figure (8), the combination of bonded *NSM* bars and *CFRP* jacketing displayed the best response characteristics. Jacketing with *CFRP* improved the bond conditions and restrained buckling of the reinforcements, thereby making the strength to increase approximately 20% in the specimens.

The specimen *C*5 attained the maximum flexural resistance, which was nearly double that of the control specimen. Also, at large lateral displacement, the column with the *CFRP* jacket showed a more ductile response due to an improved confinement, see Figures (7d) and (7e). Therefore, it seems that the combination of *NSM* flexural strengthening and *CFRP* jacketing is a viable means for increasing the strength of columns. A similar result is observed by Bournas and Triantafillou [14].

3.3. Strains in NSM Rods and Reinforcement

In strengthened columns compared with unstrengthened column, yielding of reinforcement bar took place later. Also, in column *C*2, *NSM* rods achieved tensile strain values close to the ultimate rupture strain of the *NSM*. This indicated that the rehabilitation schemes used for specimens *C*2, *C*3, *C*4 and *C*5 were successful in providing flexure strength of columns and delay in yield of reinforcement bars.

Figure (9) illustrates the relationship between the lateral displacement applied to the column and the strain in the strain-gauge *SG*1, for the columns *C*2 and *C*3. Due to carrying compression forces by concrete material, the maximum compressive strain in the *NSM* rod was about half of the value recorded in tension. Relationships similar to those depicted in Figure (9) were obtained for other specimens.

3.4. Ductility

The displacement ductility for all specimens are calculated from the envelope curves and is given in Table (3). The displacement ductility is defined as the displacement at 80% of the maximum lateral load in the softening branch divided by the yield displacement ($\mu = \Delta u/\Delta y$). The yield displacement was evaluated when steel bars were yielded and measured by strain gauges.

The displacement ductility of the unstrengthened control columns, *C*1, is 2.4. Among the retrofitted columns, column *C*2 has a ductility ratio of 3.2 and column *C*3 which was retrofitted by 4 *NSM* rods with a ductility ratio of 2.8. Columns *C*4 and *C*5 were retrofitted by both jacketing and *NSM* embedment and have the largest ductility ratios of 4.3 and 4.2, respectively. As a result, the combination of *NSM* bar and *CFRP* jacketing is the best way for increasing the ductility. Also, the displacement ductility of specimen *C*2 with the lower *NSM* bars is higher than that of *C*3. Comparing the displacement ductility of specimens shown in Table (3), indicates that increasing the ratio of *NSM* decreases the ductility of column.

3.5. Energy Dissipation Capacity

The energy dissipated by the specimen was

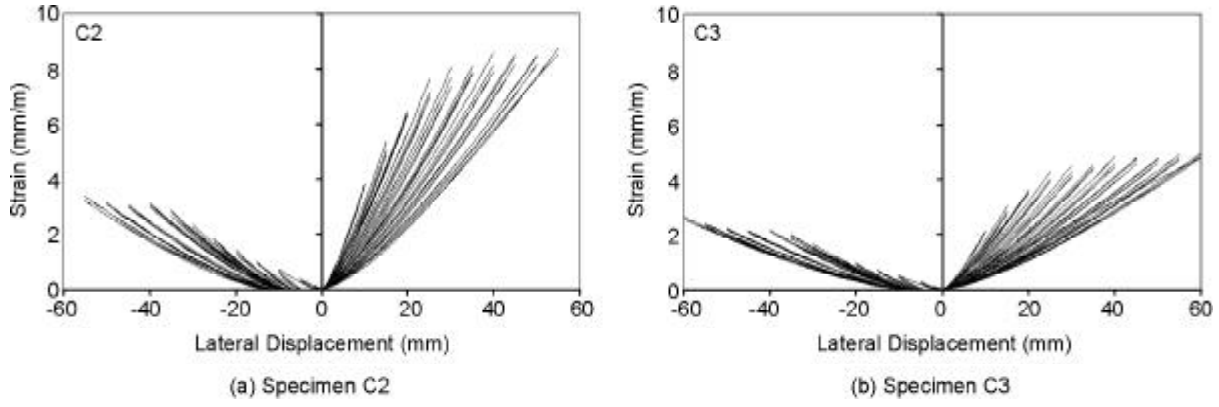

Figure 9. Measured strain in NSM rod.

obtained by calculating the area enclosed by the corresponding load-displacement hysteretic loop. Figure (10) shows the cumulative dissipated energy versus the cumulative lateral displacement for all models. The wobbles in the energy dissipation curves are caused by the elastic energy release at the unloading paths of each cycle.

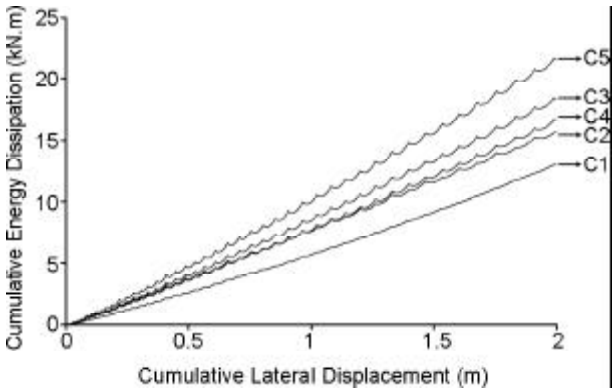

Figure 10. Energy dissipation of columns.

The results of energy dissipation clearly demonstrated that retrofitted specimens dissipated more energy than the control specimen and *NSM* rod embedment causes an increase in toughness of columns and therefore, are very effective for retrofitting of *RC* columns. Comparing the energy dissipated capacity for specimens *C*2 and *C*3 indicates that the cumulative energy dissipated capacity for specimen *C*3 with the larger number of *NSM* bar is higher than specimen *C*2 as can be seen in Figure (10). Therefore, increasing the number of *NSM* bar increases the dissipated energy capacity. Specimen *C*5 which was strengthened using *NSM* rods and *CFRP* jacket had higher energy dissipated capacity as compared to column *C*3 which was strengthened using *NSM* bars only. The energy dissipated by this specimen was nearly two times higher than the corresponding values for the unretrofitted column. Therefore, it seems that the combination of *NSM* flexural strengthening and *CFRP* jacket is an appropriate means for increasing the energy dissipated capacity.

3.6. Stiffness Degradation

The stiffness degradation based on the envelope curves are shown in Figure (11), in which K_0 is the initial stiffness, K_i is the instantaneous secant

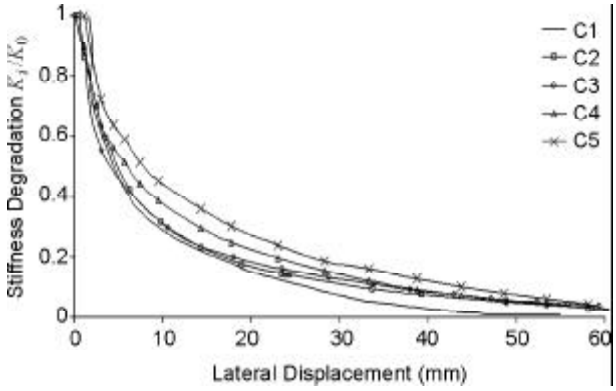

Figure 11. Stiffness degradation of columns.

stiffness at a certain displacement, and K_i / K_0 is the percentage of remaining stiffness relative to the initial stiffness K_0.

Before reaching ultimate load carrying capacity, the stiffness degradation of specimens *C*4 and *C*5 were smaller than that of the others and the stiffness degradation of *C*2 and *C*3 was similar to column *C*1. After that, the unretrofitted column deteriorated faster in terms of stiffness than the retrofitted columns. This is reasonable because more serious deterioration occurred in the compression zone of the unretrofitted columns after the onset of the peak strength as compared with that in the retrofitted columns. It is also demonstrated that the deterioration of concrete was similar in both the unretrofitted and retrofitted columns before the onset of the peak strength. Therefore, it is evident that the retrofit methods slowed down the degradation of the force-displacement curve in descending branch.

After reaching peak strength, the stiffness degradation was generally similar among all the retrofitted columns. As a result, it can be concluded that the *NSM* embedment was as effective as jacketing in maintaining the integrity of the columns.

4. Analytical Modeling

4.1. Basis for Design Approach

Theoretical flexural capacity of a *NSM* strengthened concrete column is determined based on strain compatibility and internal force equilibrium. Figure (12) illustrates the assumed basic analytical conditions of internal strain, stress, and resultant force for a *RC* column strengthened with *NSM* bars. The strengthening design approach is based on iteration procedure in which a concrete strain at failure is first

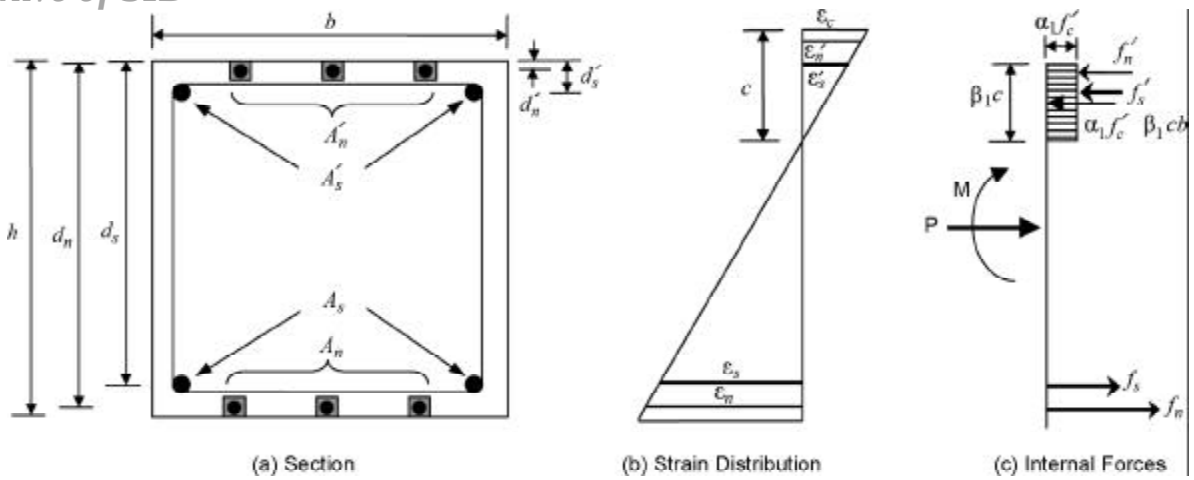

Figure 12. Strain and stress condition of RC section strengthened with NSM FRP rods.

assumed and the depth of neutral axis is determined by trial and error. From Figure (12), the following assumptions are implicit: strain varies linearly through the cross section; the section is initially uncracked; perfect bond exists between the steel and *NSM* reinforcements and concrete; the concrete strain at compression failure is 0.003; the stress-strain relationship of concrete is based on the parabolic equation proposed by Todeschini et al [15]; the *NSM* stress-strain behavior is assumed to be elastic; and the steel stress-strain behavior is assumed to be elastic-plastic. The analytical procedure used to determine the moment capacity can be summarized as follows:

1) Assume the concrete strain at failure and the depth of neutral axis.
2) The parameters that define the equivalent stress block are defined as follows [15]:

$$\beta_1 = \frac{4\varepsilon'_c - \varepsilon_c}{6\varepsilon'_c - 2\varepsilon_c} \quad (1)$$

$$\alpha_1 = \frac{3\varepsilon'_c\varepsilon_c - \varepsilon_c^2}{3\beta_1\varepsilon'^2_c} \quad (2)$$

$$\varepsilon'_c = \frac{1.71\, f'_c}{E_c} \quad (3)$$

3) The strain of steel and *FRP* reinforcement are determined utilizing compatibility of the section.
4) The stress of steel and *FRP* reinforcement is determined from the constitutive laws of the materials.
5) The depth of the neutral axis is then determined utilizing equilibrium and accounting for the axial load, *P*.
6) If the calculated value of the neutral axis, *c* does not match the assumed one, another value is assumed and the process is continued until the two values converge. The flexural capacity of the section is determined as follows:

$$M = \alpha_1 f'_c \beta_1 cb(\frac{h}{2} - \frac{\beta_1 c}{2}) + A'_s f'_s(\frac{h}{2} - d'_s) + A_s f_s(d_s - \frac{h}{2}) + A'_n f'_n(\frac{h}{2} - d'_n) + A_n f_n(d_n - \frac{h}{2}) \quad (4)$$

4.2. Analytical Results

A computer program was coded to carry out the analytical procedure. Sectional geometry and mechanical properties of concrete, steel, and *NSM* bar were used as input data in the analysis. The predicted and experimental results are given in Table (4). From this table, it can be seen that the proposed analysis gives reasonable predictions for the columns' flexural capacity. The difference between the predicted and measured strength may be ascribed to a variation in the material's strength. All predicted strengths were within 6% error band which demonstrates the ability of the proposed analysis to provide an accurate prediction for the flexural capacity of *RC* columns strengthened with

Table 4. Comparison between analytical predictions and experimental results.

Specimen	$M_{experimental}$ (kN.m)	$M_{analytical}$ (kN.m)	Error [a] (%)
C2	26.4	27	+2.2
C3	34.6	32.5	-6.1

[a]Error (%) = $(M_{analytical} - M_{experimental})/ M_{experimental}$ x100

NSM bars. Figure (13) shows typical interaction curves for specimens *C*2 and *C*3 strengthened with *NSM* bars.

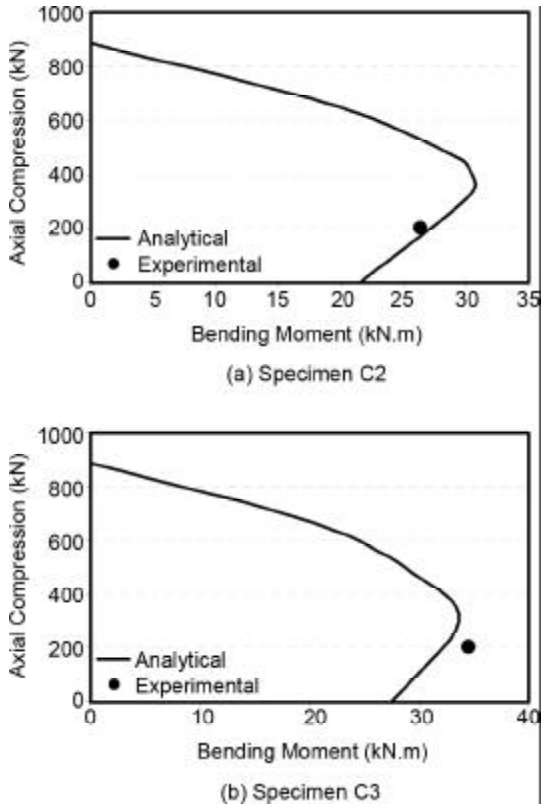

Figure 13. Typical axial load-bending moment interaction curves.

5. Conclusions

In this research, a new method of strengthening based on embedding *NSM* rods into the grooves on the cover of concrete to retrofit *RC* columns, has been investigated. The results from an experimental study, which included five *RC* square columns, were represented and discussed. These columns were strengthened with different ratio of *NSM* rods and *CFRP* sheets and were tested under cyclic lateral loads and constant axial load. Based on the results of the experimental program, the following conclusions are considered:

- *NSM* rod is very promising for increasing the flexural resistance of *RC* columns subjected to seismic loads and failing in bending.
- Increasing the number of *NSM* bars increases the lateral strength capacity and energy dissipation capacity.
- The displacement ductility of specimen with the lower *NSM* bars is higher than specimen with higher *NSM* bars.
- Using the *CFRP* jacketing with *NSM* rods, increases the ductility of column. This prevents possible instability of the rods under compression and stops splitting cracks of the grout when rods are in tension.
- This method significantly improved the cumulative energy dissipation capacity of specimens. When the *NSM* ratio was increased, the energy dissipation capacity was also increased.
- This technique could be used to delay the stiffness degradation of the reinforced concrete columns. After reaching peak strength, the stiffness degradation of retrofitted columns was slower than the unretrofitted column. Therefore, this method was effective in delaying the concrete deterioration and to prevent the buckling of longitudinal reinforcement.
- The most appropriate strengthening technique for both flexural strengthening and ductility of columns was found to be the use of *NSM* rods over the height of the column for enhancing the strength and the additional confinement using *CFRP* jacketing to increase the ductility. The conclusions made above are in perfect agreement, with those made by Bournas and Triantafillou [14].

Acknowledgments

The experimental tests described in this paper were conducted in the structural laboratory at the International Institute of Earthquake Engineering and Seismology (*IIEES*). The authors are grateful to *IIEES* for the support.

References

1. Park, R. (2001). "Improving the Resistance of Structures to Earthquakes", Bulletin of the New-Zealand Society for Earthquake Engineering, **34**(1), 1-39.

2. Saadatmanesh, H., Ehsani, M.R., and Li, M.W. (1994). "Strength and Ductility of Concrete Columns Externally Reinforced with Fiber Composite Straps", *ACI Structural Journal*, **91**(4), 434-447.

3. Saadatmanesh, H., Ehsani, M., and Jin, L. (1996). Seismic Strengthening of Circular Bridge Pier Models with Fiber Composites", *ACI Structural Journal*, **93**(6), 639-647.

4. Seible, F., Priestley, M.J.N., Hegemier, G.A., and

Innamorato, D. (1997). "Seismic Retrofit of RC Columns with Continuous Carbon Fiber Jackets", *Journal of Composite for Construction*, **1**(2), 52-62.

5. Mirmiran, A., Shahawy, M., Samaan, M., El Echary, H., Mastrapa, J.C. and Pico, O. (1998). "Effect of Column Parameters on FRP-Confined Concrete", *Journal of Composite for Construction*, **2**(4), 175-185.

6. Saafi, M., Toutanji, H.A., and Li, Z. (1999). "Behavior of Concrete Columns Confined with Fiber Reinforced Polymer Tubes", *ACI Material Journal*, **96**(4), 500-509.

7. Teng, J., Chen, J., Smith, S., and Lam, L. (2002). "*FRP-Strengthened RC Structures*", Wiley, London.

8. De Lorenzis, L. and Nanni, A. (2002). "Bond between NSM Fiber-Reinforced Polymer Rods and Concrete in Structural Strengthening", *ACI Structural Journal*, **99**(2), 123-132.

9. Taljsten, B., Carolin, A., and Nordin, H. (2003). Concrete Structures Strengthened with Near Surface Mounted Reinforcement of CFRP", *Advance in Structural Engineering*, **6**(3), 201-213.

10. Hassan, T. and Rizkalla, S. (2004). "Bond Mechanism of Near-Surface-Mounted Fiber-Reinforced Polymer Bars for Flexural Strengthening of Concrete Structures", *ACI Structural Journal* , **101**(6), 830-839.

11. El-Hacha, R. and Rizkalla, S.H. (2004). "Near-Surface-Mounted Fiber-Reinforced Polymer Reinforcements for Flexural Strengthening of Concrete Structures", *ACI Structural Journal*, **101**(5), 717-726.

12. Barros, J.A.O., Ferreira, D.R.S.M., Fortes, A.S., and Dias, S.J.E. (2006). "Assessing the Effectiveness of Embedding CFRP Laminates in The Near Surface for Structural Strengthening", *Construction and Building Materials*, **20**(7), 478-491.

13. Barros, J.A.O., Varma, R.K., Sena-Cruz, J.M., and Azevedo, A.F.M. (2008). "Near Surface Mounted CFRP Strips for the Flexural Strengthening of RC Columns: Experimental and Numerical Research", *Engineering Structures*, **30**(2), 3412-3425.

14. Bournas, D.A. and Triantafillou, T.C. (2009). "Flexural Strengthening of Reinforced Concrete Columns with Near Surface-Mounted FRP or Stainless Steel", *ACI Structural Journal*, **106**(4), 495-505.

15. Todeschini, C., Bianchini, A.C., and Kesler, C.E. (1964). "Behavior of Concrete Columns Reinforced with Strength Steels", *ACI Journal, Proceedings*, **61**(6), 701-716.

Notation

A_n = Area of tension *NSM* reinforcement
A'_n = Area of compression *NSM* reinforcement
A_s = Area of tension steel reinforcement
A'_s = Area of compression steel reinforcement
b = Width of the section
c = Depth of neutral axis
d_n = Depth to tension *NSM* reinforcement centroid
d'_n = Depth to compression *NSM* reinforcement centroid
d_s = Depth to tension steel reinforcement centroid
d'_s = Depth to compression steel reinforcement centroid
E_c = Elastic modulus of concrete in compression
f'_c = Compressive strength of concrete
f_n = Stress level developed in tension *NSM* reinforcement
f'_n = Stress level developed in compression *NSM* reinforcement
f_s = Stress level developed in tension steel reinforcement
f'_s = Stress level developed in compression steel reinforcement
h = Height of column
M = Moment on column
P = Axial force on column
α_1 = Multiplier on concrete strength to determine the equivalent concrete strength of an equivalent rectangular stress block
β_1 = Multiplier on c to determine the depth of an equivalent rectangular stress block
ε_c = Compressive strain level in the concrete
ε'_c = Strain level in the concrete corresponding to the peak concrete stress
ε_n = Strain level in tension *NSM* reinforcement
ε'_n = Strain level in compression *NSM* reinforcement
ε_s = Strain level in tension steel reinforcement
ε'_s = Strain level in compression steel reinforcement.